A Revenue-Adequate Market Design for Grid-Enhancing Technologies

Xinyang Rui[a], Omid Mirzapour[a] and Mostafa Ardakani[a,*]

[a]Department of Electrical and Computer Engineering, University of Utah, , Salt Lake City, UT, 84112, USA

ARTICLE INFO

Keywords:
Electricity market
Grid-enhancing technologies
Power flow control
Transmission investment incentive
Power system flexibility
Transfer capability

ABSTRACT

Grid-enhancing technologies (GETs) are expected to be vital for upgrading the transmission system to accommodate higher levels of penetration from renewable energy sources (RES). Proper financial incentives are key to facilitating the deployment of GETs. This paper presents a market model based on co-optimizing GET setpoints alongside generation dispatch in power system operation. The dual variables associated with GET constraints serve as the marginal price for GET operation. GET owners receive payments based on this marginal price and GET setpoints. Proof of revenue adequacy for the proposed market design is presented. Simulation studies on two IEEE test cases show that the market design effectively rewards efficient GET operation and results in substantially higher payments than those from a regulated rate of return. The results suggest that the adoption of a market design, similar to what is presented in this paper, for GETs can lead to GETs proliferation and bring unprecedented levels of efficiency to transmission network utilization. The developed model is linear and scales well for large real-world systems. However, the adoption of the design will require regulatory changes and rulemaking by the Federal Energy Regulatory Agency.

Nomenclature

Indices

$\mathrm{fr}(k)$ The "from" bus of branch k

$\mathrm{to}(k)$ The "to" bus of branch k

g Generator

i, j GET deployment

$k(i)$ Transmission branch k with GET i deployed

k Transmission branch

$n(g)$ Bus n to which generator g is connected

n Bus

Parameters

$\mathbf{f}^{\max}$ Thermal capacities of transmission lines

θ_i^{PST} Maximum phase shift by PST deployment i

$\mathbf{0}$ Vector of zeros

$\mathbf{1}$ Vector of ones

* Corresponding Author
xinyang.rui@utah.edu (X. Rui); omid.mirzapour@utah.edu (O. Mirzapour); mostafa.ardakani@utah.edu (M. Ardakani)
ORCID(s): 0000-0002-0517-6721 (X. Rui); 0000-0001-6063-2534 (O. Mirzapour); 0000-0002-5770-8291 (M. Ardakani)

$\mathbf{\Delta f}^{\max}$ GET nodal injections upper bound

$\mathbf{\Gamma}$ Generator placement matrix

$\mathbf{\Phi}$ Injection shift factor matrix

$\mathbf{\Psi}$ GET placement matrix

$\mathbf{A}$ Incidence matrix

$\mathbf{c}$ Linear costs of generators

$\mathbf{d}$ Vector of nodal Demands

$\mathbf{p}^{\max}$ Maximum output of generator g

$\mathbf{p}^{\min}$ Minimum output of generators

b_k Susceptance of branch k

C^{FACTS} Unit cost of FACTS devices

C^{PST} Unit cost of PSTs

C_i^{FACTS} Cost of FACTS deployment i

C_i^{PST} Cost of PST deployment i

S_i^{FACTS} Rating of FACTS deployment i

$V_i^{\max}$ Maximum voltage injection by FACTS deployment i

Sets

$\mathcal{G}$ Set of GET deployments

G Set of generators

K Set of transmission branches

N Set of buses

Variables

λ System-wide marginal price

θ_n Voltage angle of bus n

$\tilde{\lambda}$ Locational marginal prices

$\boldsymbol{\alpha}^+, \boldsymbol{\alpha}^-$ Generator capacity prices

$\boldsymbol{\beta}^+, \boldsymbol{\beta}^-$ Flowgate marginal prices

$\mathbf{\Delta f}$ GET nodal injections

$\boldsymbol{\tau}^+, \boldsymbol{\tau}^-$ GET marginal prices

$\mathbf{f}$ (Partial) active power flows

$\mathbf{p}$ Active power output of generators

GR_i Revenue of GET deployment i

TGR Total GET revenue

TLP Total load payment

TPR Total production (generation) revenue

TTR Total transmission revenue

1. Introduction

The transmission system needs upgrades to alleviate congestion and accommodate the increasing penetration from renewable energy sources (RES). Grid-enhancing technologies (GETs) are an efficient alternative to constructing new transmission lines to enhance the grid's transfer capability. GETs include a range of hardware and software tools that improve the utilization of the existing system [1]. Prominent examples of GET include flexible AC transmission systems (FACTS), phase-shifting transformers (PSTs), dynamic line rating (DLR), and transmission switching (TS) [2]. These technologies can alter key transmission parameters and alleviate transmission system constraints to facilitate more cost-efficient generation dispatch and pave the way for a cleaner electricity sector with reduced carbon emission [3].

Despite the relative maturity of the technology, GET adoption remains rather limited [4]. One of the main challenges hindering GET deployments is the lack of proper financial incentives [1, 5]. GETs are currently treated as a part of a regulated monopoly transmission network. Similar to any other prudent transmission investment, GETs will receive a regulated rate of return (RoR). Under such a structure, the return is calculated based on investments, thus creating a preference towards transmission system upgrades that involve higher investments. Therefore, from the investor's perspective, GET deployments, which involve smaller capital expenditures compared to transmission expansion projects, are negatively affected [6, 7, 1].

To overcome this challenge, several performance-based compensation mechanisms have been proposed to incentivize GET investments. One method proposed to allocate financial transmission rights (FTRs) to GET investors [4]. The FTRs would enable the investors to collect market-based payments or trade the allocated rights in long-term markets, including FTR auctions and secondary markets [8]. However, the FTR's downside is the loose link between the revenue allocation and real-time operation of GETs in the short-term markets. Therefore, there will be a need for additional processes to ensure efficient operation in real time.

The second key approach is to reward transmission investments with the benefits they create. Previous studies have proposed such an approach as a performance-based incentive for transmission expansion projects [9, 10]. However, proposals regarding GET investments are relatively limited. Ref. [11] presents a method that uses the benefits of FACTS operation as financial compensation for investments, with benefits measured by changes in generation and demand surpluses, as well as congestion rent. The WATT Coalition proposed the shared-savings incentives for GETs [12] in recent years, allowing asset owners to receive a portion of the savings created by GET deployments. A clear drawback of such proposed methods is that savings calculation requires a base case solution without considering GETs, leading to extra computational burden. Moreover, the allocation of savings to multiple GETs may not be straightforward.

A third approach is to calculate a marginal price for transmission projects based on the dual solution of power system optimization problems. For this approach, transmission infrastructures are viewed as a resource, and the dual variables serve as measurements of marginal value. An example of this approach for transmission expansion is the use of flowgate marginal prices (FMP) to compensate transmission companies [13, 14, 15]. Ref. [16] presents a method for GETs following this approach which uses dual variables from DC power flow, referred to as the susceptance price, as a price signal for variance-impedance FACTS operations. The proposed method, although straightforward, has the major drawback of providing no revenue adequacy guarantee.

Based on the literature review of proposed incentive mechanisms for GETs, the existing literature lacks a performance-based market design that considers the full integration of GET operation into power system operation models while ensuring revenue adequacy. Co-optimizing GET operations with generation dispatch is essential for the full realization of their benefits. Various modeling techniques are developed in the literature to facilitate the integration of GETs into power system operation models [17, 18]. These models must be included in energy and market management systems (EMS/MMS) to adjust GET setpoints and incorporate their influence in market-clearing processes. Therefore, a desirable approach would be to calculate a price signal for GETs alongside the locational marginal price, which is used to settle generation revenue and load payment. This paper fills the research gap by proposing a market design for two main types of GETs, VSC-based series FACTS and PSTs. The proposed market design rewards asset owners based on a price signal. This price is obtained from the dual solution of DC optimal power flow (DCOPF) co-optimizing GET setpoints, and measures the marginal value of GET operations. The DCOPF model in this paper fully considers the operation constraints of GETs. The approach leading to the proposed market design can be demonstrated by Fig 1.

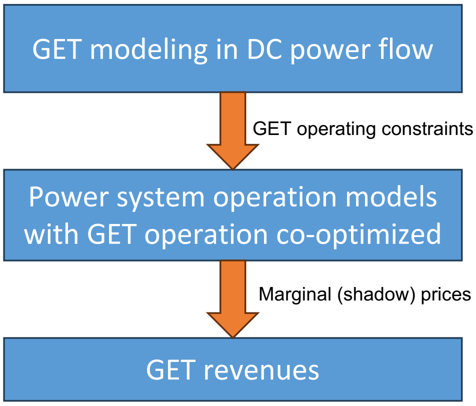

Figure 1: GET revenues in electricity markets considering GET operations

The main contributions of this paper are summarized as follows:

1. To incentivize efficient GET investments and optimal operations, this paper proposes a market design that provides payoffs to GET owners based on marginal prices associated with GET revenue constraints. It allows full market integration of GET operations by settling the payoffs simultaneously with other payments for generation, load, and transmission.
2. Revenue adequacy of the proposed market design is proved, by showing that the total congestion rent is sufficient to cover GETs payments and prior transmission commitments.

This paper considers prominent GETs that provide power flow control capabilities with linear models. Linear GET models are compatible with the existing market operation software, making the implementation straightforward. The proposed market design aligns incentives with performance, where every profitable investment will require efficient planning and operation.

The remainder of the paper is organized as follows. Section 2 presents the mathematical modeling of GETs, the proposed market design, and the proof of revenue adequacy. Numerical results on two test systems are shown in Section 3. Finally, Section 4 concludes the paper.

2. Methodology

2.1. GET operation modeling

Two prominent types of GET, including VSC-based series FACTS devices and PSTs, are included in this paper. These technologies can help alleviate congestion through their power flow control capabilities. The nodal power injection model [19] of GETs is employed in this paper. This modeling technique separates the term associated with GET operations from the term calculated using the original line susceptance in the power flow equations, thus allowing the application of the injection shift factors (ISFs) without needing modification [17]. The injection pair model is demonstrated in Fig 2.

The operation constraints of static synchronous series compensators (SSSC) and unified power flow controllers (UPFC), which are both prominent FACTS technologies, in DC power flow are formulated as follows [17] for line $k(i)$ equipped with GETs:

$$\tilde{f}_{k(i)} = f_{k(i)} + \Delta f_i = b_{k(i)}(\theta_{\mathrm{to}(k(i))} - \theta_{\mathrm{fr}(k(i))}) + \Delta f_i, \tag{1}$$

$$-V_i^{\max} b_{k(i)} \le \Delta f_i \le V_i^{\max} b_{k(i)}, \tag{2}$$

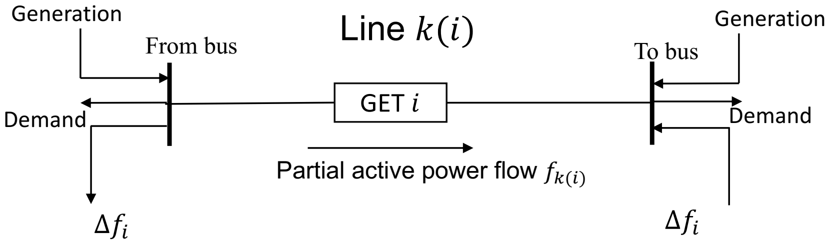

Figure 2: Nodal power injection model of GETs

where $\tilde{f}_{k(i)}$ is the active power flow on line $k(i)$. Note that $f_{k(i)}$ represents only the partial flow calculated using $b-\theta$ based on the original line susceptance. Variable Δf_i is the nodal injection from GET deployment i. It is also worth noting that the power flow control functionalities are not increasing line capacities, as the thermal capacity limits are enforced on the full power flow, as demonstrated in the problem formulation shown later in this section.

PSTs can be modeled similarly in DC power flow. The constraints are presented as follows [18]:

$$-\theta_i^{\max} b_{k(i)} \leq \Delta f_i \leq \theta_i^{\max} b_{k(i)}. \tag{3}$$

Overall, based on (2) and (3), the modeling of the GETs considered in this paper allows a unified operating constraint formulation on their injection pairs, which is presented as follows:

$$-\Delta f_i^{\max} \leq \Delta f_i \leq \Delta f_i^{\max}. \tag{4}$$

Furthermore, the modeling approach preserves both linearity and the continuum of DCOPF. Granted, other types of GETs have different models that may not be compatible with the operation model formulation in this paper. However, the model in this paper effectively demonstrates the proposed mechanism with prominent power flow controllers.

2.2. Market design

Based on the linear modeling presented in the previous subsection, the DCOPF problem with ISFs considering GET operation is formulated as follows:

P0 :

$$\text{minimize } \mathbf{c}^{\mathrm{T}}\mathbf{p} \tag{5}$$

s.t.

$$\mathbf{p}^{\min} \leq \mathbf{p} \leq \mathbf{p}^{\max}, \qquad (\boldsymbol{\alpha}^-, \boldsymbol{\alpha}^+) \tag{6}$$

$$\mathbf{f} = \boldsymbol{\Phi}(\boldsymbol{\Gamma}\mathbf{p} - \mathbf{d} - \mathbf{A}^{\mathrm{T}}\boldsymbol{\Psi}\boldsymbol{\Delta}\mathbf{f}), \qquad (\boldsymbol{\sigma}) \tag{7}$$

$$-\mathbf{f}^{\max} \leq \mathbf{f} + \boldsymbol{\Psi}\boldsymbol{\Delta}\mathbf{f} \leq \mathbf{f}^{\max}, \qquad (\boldsymbol{\beta}^-, \boldsymbol{\beta}^+) \tag{8}$$

$$\mathbf{1}_g^{\mathrm{T}}\mathbf{p} - \mathbf{1}_n^{\mathrm{T}}\mathbf{d} = 0, \qquad (\lambda) \tag{9}$$

$$-\boldsymbol{\Delta}\mathbf{f}^{\max} \leq \boldsymbol{\Delta}\mathbf{f} \leq \boldsymbol{\Delta}\mathbf{f}^{\max}. \qquad (\boldsymbol{\tau}^-, \boldsymbol{\tau}^+) \tag{10}$$

The variables shown in parenthesis are the dual variables associated with the corresponding constraints. Details of certain matrices in P0 are shown in Appendix A. The objective function (5) minimizes the total production cost. Constraints on generating unit outputs are presented in (6). The impact of nodal power injection on power flows is calculated using ISFs as shown in (7). Constraint (8) enforces the thermal capacity limits on transmission lines. System-wide power balance is shown in (9). Finally, GET operating ranges are shown in (10).

Dual variables $\boldsymbol{\tau}^-$ and $\boldsymbol{\tau}^+$ can be used as marginal prices for GETs, and they measure the marginal savings in total production cost achieved by incremental changes of the GET operating limits shown in (10). Therefore, in the proposed market design, the GET revenues for individual GET deployments and the total GET revenue (TGR) are formulated as follows:

$$GR_i = (\tau_i^{+*} - \tau_i^{+*})\Delta f_i^*, \tag{11}$$

$$TGR = \sum GR_i = (\boldsymbol{\tau}^{+*} - \boldsymbol{\tau}^{-*})^{\mathrm{T}} \boldsymbol{\Delta}\mathbf{f}^*. \tag{12}$$

Equations (11) and (12) show that GET revenues are calculated using marginal values, which are the dual variables, and quantities, which are GET nodal injections. They are consistent with the market clearing processes with DCOPF, where marginal prices are utilized for settling payments. The formulation of GET revenues in this paper has some desirable properties presented with the lemmas below.

Lemma 1: GET revenues are non-negative.

Proof: According to complementary slackness, for GET deployment i, we have:

$$\tau_i^{+*}(\Delta f_i^* - \Delta f_i^{\max}) = 0, \tag{13}$$

$$\tau_i^{-*}(\Delta f_i^{\max} + \Delta f_i^*) = 0. \tag{14}$$

Therefore, (11)-(12) can be alternatively shown as:

$$GR_i = (\tau_i^{+*} + \tau_i^{-*})\Delta f_i^{\max}, \tag{15}$$

$$TGR = (\boldsymbol{\tau}^{+*} + \boldsymbol{\tau}^{-*})^{\mathrm{T}} \boldsymbol{\Delta}\mathbf{f}^{\max}. \tag{16}$$

Additionally, dual feasibility states that:

$$\tau_i^{+*} \geq 0, \tag{17}$$

$$\tau_i^{-*} \geq 0. \tag{18}$$

Therefore, using the equations above, we have:

$$GR_i \geq 0, \tag{19}$$

$$TGR \geq 0. \tag{20}$$

Lemma 1 is, thus, proved.

Lemma 2: GR_i is zero when GET operating constraint of deployment i is not binding.

Proof: If (10) is not binding for GET deployment i, then based on (13)-(14), we have:

$$\tau_i^{+*} = \tau_i^{-*} = 0, \tag{21}$$

$$GR_i = 0. \tag{22}$$

Lemma 2 means GETs not operating at limits do not collect payments. This is justified as GETs have zero or negligible operating costs. GETs not operating at a limit implies that the asset does not contribute to congestion reduction, and thus, is not valuable in that particular system state. Thus, the asset should not collect payment. Only when the asset is operating at a limit can we conclude that it has contributed to an efficient dispatch and additional capacity would be desired. It is only in such circumstances that a GET installation will receive a non-zero payment. This property of the proposed market design helps to ensure market efficiency regarding GET planning, as redundant investment in GET deployments likely results in zero payoffs.

Lemma 3: TGR will not exceed the savings created by GET operations.

Proof: The savings is essentially the difference between the objective function value at optimality between P0 and the base case DCOPF without any GETs. We first consider the following optimization problem:

P1 :

$$\text{minimize } \mathbf{c}^{\mathrm{T}}\mathbf{p} \tag{23}$$

s.t.

(6), (7), (8), (9)

$$-\mathbf{0} \leq \mathbf{\Delta f} \leq \mathbf{0} \tag{24}$$

P1 is equivalent to a base case DCOPF. Note that the variables and constraints regarding GET operations are still included in the formulation, only with the bounds set at zero as shown in (24). The LaGrange dual problems of P0 and P1 are presented as follows:

$\tilde{\text{P0}}$:

$$\begin{aligned}&\text{maximize } q(\boldsymbol{\gamma}) = -\boldsymbol{\alpha}^{+\mathrm{T}}\mathbf{p}^{\max} + \boldsymbol{\alpha}^{-\mathrm{T}}\mathbf{p}^{\min} + \boldsymbol{\sigma}^{\mathrm{T}}\mathbf{\Phi d}\\&- \lambda\mathbf{1}_n^{\mathrm{T}}\mathbf{d} - \boldsymbol{\beta}^{+\mathrm{T}}\mathbf{f}^{\max} - \boldsymbol{\beta}^{-\mathrm{T}}\mathbf{f}^{\max}\\&- \boldsymbol{\tau}^{+\mathrm{T}}\mathbf{\Delta f}^{\max} - \boldsymbol{\tau}^{-\mathrm{T}}\mathbf{\Delta f}^{\max}\end{aligned} \tag{25}$$

s.t.

$$(\boldsymbol{\alpha}^{-} - \boldsymbol{\alpha}^{+}) - \mathbf{c} + \mathbf{\Gamma}^{\mathrm{T}}\mathbf{\Phi}^{\mathrm{T}}\boldsymbol{\sigma} - \lambda\mathbf{1}_g \leq \mathbf{0} \tag{26}$$

$$(\boldsymbol{\beta}^{+} - \boldsymbol{\beta}^{-}) + \boldsymbol{\sigma} = \mathbf{0} \tag{27}$$

$$\mathbf{\Psi}^{\mathrm{T}}(\boldsymbol{\beta}^{+} - \boldsymbol{\beta}^{-}) + \mathbf{\Psi}^{\mathrm{T}}\mathbf{A}\mathbf{\Phi}^{\mathrm{T}}\boldsymbol{\sigma} + (\boldsymbol{\tau}^{+} - \boldsymbol{\tau}^{-}) = \mathbf{0} \tag{28}$$

$\tilde{\text{P1}}$:

$$\begin{aligned}&\text{maximize } q_1(\boldsymbol{\gamma}) = -\boldsymbol{\alpha}^{+\mathrm{T}}\mathbf{p}^{\max} + \boldsymbol{\alpha}^{-\mathrm{T}}\mathbf{p}^{\min} + \boldsymbol{\sigma}^{\mathrm{T}}\mathbf{\Phi d}\\&- \lambda\mathbf{1}_n^{\mathrm{T}}\mathbf{d} - \boldsymbol{\beta}^{+\mathrm{T}}\mathbf{f}^{\max} - \boldsymbol{\beta}^{-\mathrm{T}}\mathbf{f}^{\max}\end{aligned} \tag{29}$$

s.t.

(26), (27), (28).

where $q(\cdot)$ and $q_1(\cdot)$ denote the dual objectives and $\boldsymbol{\gamma}$ represents the dual variables. Let $\boldsymbol{\gamma}^*$ and $\boldsymbol{\gamma}_1^*$ represent the sets of dual variables of P0 and P1 at optimality, respectively. Based on strong duality, the savings can be derived using the difference between the dual optimal objectives of P0 and P1. Therefore, Lemma 3 can be equivalently presented as the following inequality:

$$TGR = (\boldsymbol{\tau}^{+*} + \boldsymbol{\tau}^{-*})^{\mathrm{T}}\mathbf{\Delta f}^{\max} \leq q_1(\boldsymbol{\gamma}_1^*) - q(\boldsymbol{\gamma}^*). \tag{30}$$

To prove (30), we first further derive its right-hand side as:

$$q_1(\boldsymbol{\gamma}_1^*) - q_1(\boldsymbol{\gamma}^*) + (\boldsymbol{\tau}^{+*} + \boldsymbol{\tau}^{-*})^{\mathrm{T}}\mathbf{\Delta f}^{\max}. \tag{31}$$

Therefore, Lemma 3 can be proved if the following inequality holds:

$$q_1(\boldsymbol{\gamma}^*) \leq q_1(\boldsymbol{\gamma}_1^*). \tag{32}$$

As shown in the problem formulations, $\tilde{\text{P1}}$ and $\tilde{\text{P0}}$ share the same constraints and, thus, the same feasible region. Therefore, $\boldsymbol{\gamma}^*$ is within the feasible region of $\tilde{\text{P1}}$. Additionally, $\tilde{\text{P1}}$ is a maximization problem with $\boldsymbol{\gamma}_1^*$ being the optimal solution. Therefore, (32) is proven, which also proves Lemma 3. Lemma 3 ensures that the proposed market design does not *over-compensate* GET operations.

2.3. Revenue adequacy

Revenue adequacy implies that GET revenues in the market can be settled among participants without side payments. We present a mathematical proof to show that the congestion rent can cover the total GET revenue under the proposed market structure.

The primal and dual objectives of P0 are shown in (5) and (25), respectively. The following equation can be formulated based on strong duality:

$$q(\gamma^*) = \mathbf{c}^{\mathrm{T}}\mathbf{p}^*. \tag{33}$$

Equation (33) shows the equality between primal and dual objectives at optimality. For the rest of this section, mathematical derivations are based on optimal solutions of the primal and dual problems, and the $*$ sign is hence omitted for simplicity. Locational marginal prices (LMPs) are presented as follows:

$$\tilde{\lambda}^{\mathrm{T}} = \boldsymbol{\sigma}^{\mathrm{T}}\boldsymbol{\Phi} - \lambda\mathbf{1}_n^{\mathrm{T}}. \tag{34}$$

Eqn. (33) can be reformulated to:

$$\begin{aligned}&(\boldsymbol{\sigma}^{\mathrm{T}}\boldsymbol{\Phi}\mathbf{d} - \lambda\mathbf{1}_n^{\mathrm{T}}\mathbf{d}) - (\mathbf{c}^{\mathrm{T}}\mathbf{p} + \boldsymbol{\alpha}^{+\mathrm{T}}\mathbf{p}^{\max} - \boldsymbol{\alpha}^{-\mathrm{T}}\mathbf{p}^{\min})\\ &= \boldsymbol{\beta}^{+\mathrm{T}}\mathbf{f}^{\max} + \boldsymbol{\beta}^{-\mathrm{T}}\mathbf{f}^{\max} + \boldsymbol{\tau}^{+\mathrm{T}}\Delta\mathbf{f}^{\max} + \boldsymbol{\tau}^{-\mathrm{T}}\Delta\mathbf{f}^{\max}.\end{aligned} \tag{35}$$

The first part of the left-hand side of (35) is the total load payment (TLP) as the multiplication between $\tilde{\lambda}^{\mathrm{T}}$ and $\mathbf{d}$. Based on complementary slackness, the right-hand side of (35) is further reformulated as:

$$(\boldsymbol{\beta}^+ - \boldsymbol{\beta}^-)^{\mathrm{T}}(\mathbf{f} + \boldsymbol{\Psi}\Delta\mathbf{f}) + (\boldsymbol{\tau}^+ - \boldsymbol{\tau}^-)^{\mathrm{T}}\Delta\mathbf{f}. \tag{36}$$

The KKT conditions of P0 implies that:

$$(\boldsymbol{\alpha}^+ - \boldsymbol{\alpha}^-) + \mathbf{c} - \boldsymbol{\Gamma}^{\mathrm{T}}\boldsymbol{\Phi}^{\mathrm{T}}\boldsymbol{\sigma} + \lambda\mathbf{1}_g = 0. \tag{37}$$

Then, we have the following equation:

$$\mathbf{p}^{\mathrm{T}}(\boldsymbol{\Gamma}^{\mathrm{T}}\boldsymbol{\Phi}^{\mathrm{T}}\boldsymbol{\sigma} - \lambda\mathbf{1}_g) = \mathbf{p}^{\mathrm{T}}(\boldsymbol{\alpha}^+ - \boldsymbol{\alpha}^- + \mathbf{c}) = \mathbf{c}^{\mathrm{T}}\mathbf{p} + \boldsymbol{\alpha}^{+\mathrm{T}}\mathbf{p}^{\max} - \boldsymbol{\alpha}^{-\mathrm{T}}\mathbf{p}^{\min} \tag{38}$$

The total production revenue (TPR) can be, then, derived as:

$$\begin{aligned}&(\boldsymbol{\Gamma}\mathbf{p})^{\mathrm{T}}(\boldsymbol{\sigma}^{\mathrm{T}}\boldsymbol{\Phi} - \lambda\mathbf{1}_n^{\mathrm{T}})^{\mathrm{T}} = \mathbf{p}^{\mathrm{T}}\boldsymbol{\Gamma}^{\mathrm{T}}\boldsymbol{\Phi}^{\mathrm{T}}\boldsymbol{\sigma} - \lambda\mathbf{p}^{\mathrm{T}}\boldsymbol{\Gamma}^{\mathrm{T}}\mathbf{1}_n\\ &= \mathbf{p}^{\mathrm{T}}(\boldsymbol{\Gamma}^{\mathrm{T}}\boldsymbol{\Phi}^{\mathrm{T}}\boldsymbol{\sigma} - \lambda\mathbf{1}_g) = \mathbf{c}^{\mathrm{T}}\mathbf{p} + \boldsymbol{\alpha}^{+\mathrm{T}}\mathbf{p}^{\max} - \boldsymbol{\alpha}^{-\mathrm{T}}\mathbf{p}^{\min}\end{aligned} \tag{39}$$

Therefore, (35) can be rewritten as:

$$\mathbf{d}^{\mathrm{T}}\tilde{\lambda} - (\boldsymbol{\Gamma}\mathbf{p})^{\mathrm{T}}\tilde{\lambda} = (\boldsymbol{\beta}^+ - \boldsymbol{\beta}^-)^{\mathrm{T}}(\mathbf{f} + \boldsymbol{\Psi}\Delta\mathbf{f}) + (\boldsymbol{\tau}^+ - \boldsymbol{\tau}^-)^{\mathrm{T}}\Delta\mathbf{f}. \tag{40}$$

Additionally, total congestion rent (TCR) is formulated as follows:

$$\begin{aligned}TCR &= \tilde{\lambda}\mathbf{A}^{\mathrm{T}}(\mathbf{f} + \boldsymbol{\Psi}\Delta\mathbf{f})\\ &= -(\boldsymbol{\sigma}^{\mathrm{T}}\boldsymbol{\Phi} - \lambda\mathbf{1}_n^{\mathrm{T}})\mathbf{A}^{\mathrm{T}}(\mathbf{f} + \boldsymbol{\Psi}\Delta\mathbf{f})\\ &= -\boldsymbol{\sigma}^{\mathrm{T}}\boldsymbol{\Phi}\mathbf{A}^{\mathrm{T}}(\mathbf{f} + \boldsymbol{\Psi}\Delta\mathbf{f})\\ &= [(\boldsymbol{\beta}^+ - \boldsymbol{\beta}^-)^{\mathrm{T}}\boldsymbol{\Psi} + (\boldsymbol{\tau}^+ - \boldsymbol{\tau}^-)^{\mathrm{T}}]\Delta\mathbf{f} - \boldsymbol{\sigma}^{\mathrm{T}}\boldsymbol{\Phi}\mathbf{A}^{\mathrm{T}}\mathbf{f}\\ &= [(\boldsymbol{\beta}^+ - \boldsymbol{\beta}^-)^{\mathrm{T}}\boldsymbol{\Psi} + (\boldsymbol{\tau}^+ - \boldsymbol{\tau}^-)^{\mathrm{T}}]\Delta\mathbf{f} - \boldsymbol{\sigma}^{\mathrm{T}}\boldsymbol{\Phi}\mathbf{A}^{\mathrm{T}}\boldsymbol{\Phi}(\boldsymbol{\Gamma}\mathbf{p} - \mathbf{d} - \mathbf{A}^{\mathrm{T}}\boldsymbol{\Psi}\Delta\mathbf{f})\\ &= [(\boldsymbol{\beta}^+ - \boldsymbol{\beta}^-)^{\mathrm{T}}\boldsymbol{\Psi} + (\boldsymbol{\tau}^+ - \boldsymbol{\tau}^-)^{\mathrm{T}}]\Delta\mathbf{f} - \boldsymbol{\sigma}^{\mathrm{T}}\boldsymbol{\Phi}(\boldsymbol{\Gamma}\mathbf{p} - \mathbf{d} - \mathbf{A}^{\mathrm{T}}\boldsymbol{\Psi}\Delta\mathbf{f})\\ &= [(\boldsymbol{\beta}^+ - \boldsymbol{\beta}^-)^{\mathrm{T}}\boldsymbol{\Psi} + (\boldsymbol{\tau}^+ - \boldsymbol{\tau}^-)^{\mathrm{T}}]\Delta\mathbf{f} - \boldsymbol{\sigma}^{\mathrm{T}}\mathbf{f}\\ &= [(\boldsymbol{\beta}^+ - \boldsymbol{\beta}^-)^{\mathrm{T}}\boldsymbol{\Psi} + (\boldsymbol{\tau}^+ - \boldsymbol{\tau}^-)^{\mathrm{T}}]\Delta\mathbf{f} + (\boldsymbol{\beta}^+ - \boldsymbol{\beta}^-)^{\mathrm{T}}\mathbf{f}\\ &= (\boldsymbol{\beta}^+ - \boldsymbol{\beta}^-)^{\mathrm{T}}(\mathbf{f} + \boldsymbol{\Psi}\Delta\mathbf{f}) + (\boldsymbol{\tau}^+ - \boldsymbol{\tau}^-)^{\mathrm{T}}\Delta\mathbf{f}\end{aligned} \tag{41}$$

The derivation of (41) uses Lemma 4 shown below.
Lemma 4: The ISF matrix and incidence matrices satisfy the following:

$$\boldsymbol{\Phi}\mathbf{A}^{\mathrm{T}}\boldsymbol{\Phi} = \boldsymbol{\Phi}. \tag{42}$$

Table 1
Modifications to the 24-bus system

Branch No.	Capacity reduction (%)
A7,A21	50
A23, A27	60

Table 2
GET allocation in the 24-bus system

GET	Location	Type	Operating limit
1	A19	FACTS	0.05 pu
2	A23	FACTS	0.03 pu

Proof of Lemma 4 is presented in Appendix B.

FMPs reflect the marginal value of transmission line thermal capacities. The total transmission revenue (TTR) can, thus, be calculated as follows:

$$TTR = (\boldsymbol{\beta}^{+} - \boldsymbol{\beta}^{-})^{\mathrm{T}}(\mathbf{f} + \boldsymbol{\Psi}\boldsymbol{\Delta}\mathbf{f}). \tag{43}$$

Finally, (40) and (41) can be interpreted as:

$$TLP - TPR = TCR = TTR + TGR. \tag{44}$$

Equation (44) is essentially two equations, with the first one showing that the load payment is divided into production revenues and congestion rent. The second shows that GET revenue is part of the congestion rent and, thus, can be covered by the load payment without needing any side payments. Therefore, the revenue adequacy of the proposed market design is proved. It is also shown that under the proposed structure, existing financial transmission obligations, such as financial transmission rights, can be covered through the total transmission revenue, calculated using FMPs.

3. Numerical Studies

Numerical studies are carried out on the IEEE RTS 24-bus system [20] and the IEEE 300-bus system, with results presented in this section. The test systems vary in size thus allowing us to demonstrate the effectiveness of the proposed market design under different system topologies and various numbers of GET deployments. Both test systems are modified with increased congestion levels to better demonstrate the effectiveness of GET implementations with sizable savings. GET placement is determined following an engineering judgment that chooses lines with higher susceptance price values. It is worth noting that this study focuses on operation, and optimal GET allocation is beyond the scope of the paper. The proposed market design is illustrated through numerical results. Furthermore, the GET owners' annual revenues in the proposed market mechanism are compared with regulated returns. Results in this aspect show the effectiveness of the proposed method in incentivizing GET investments. Optimization problems are set up in Python with CVXPY [21] and solved using CPLEX 22.10.

3.1. 24-bus system

The IEEE 24-bus system data is obtained from [22]. The system is modified by reducing the thermal capacities of lines under high utilization to increase congestion. Modifications to the capacities of certain transmission branches are shown in Table 1. GET placement in the 24-bus system is shown in Table 2.

3.1.1. Single-hour operation case

We first implement P0 in a single-hour case with peak load to validate the mathematical derivations and demonstrate revenue adequacy. The results are presented in Table 3.

Furthermore, Fig. 3 demonstrates that aggregated revenues are equal to total load payments, which validates revenue adequacy.

Table 3
Results of the single-hour case

TLP	TPR	TTR	TGR
$168.252K	$124.427K	$37.065K	$6.765K

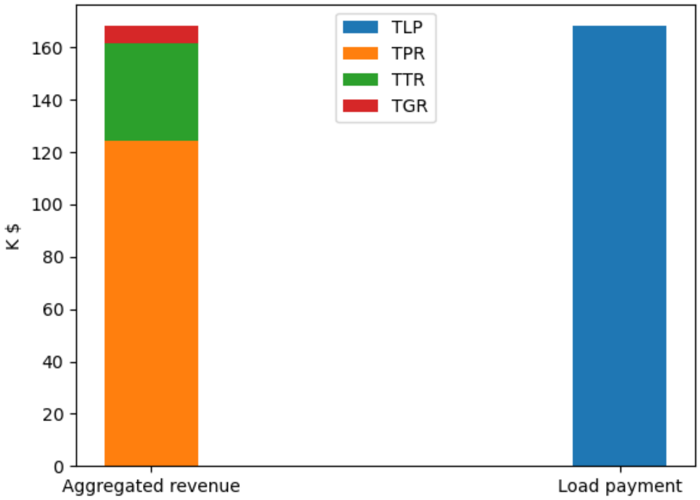

Figure 3: Comparison between revenues and load payments

3.1.2. Annualized GET revenues and comparison with RoR

Annualized returns of GET owners are estimated following the method in [23], which selects representative days of different seasons to calculate seasonal returns. This method uses Thursday, Saturday, and Sunday as representative days of the week and selects weeks 11, 25, and 51 as typical weeks of spring, summer, and winter, respectively. Note that the 11th week also represents the autumn season, as it has a similar load profile as spring. Hourly GET revenues are calculated using (12) with DCOPF results of the 216 representative time periods and provide the basis to obtain the estimated annual market revenue (AMR) of GET owners under the proposed market design.

The AMR results are compared with the annual regulated revenue (ARR) under RoR. To obtain ARR, we first calculate the device cost of GETs. The following equation is used to calculate the cost of VSC-based FACTS deployment i:

$$C_i^{\text{FACTS}} = S_i^{\text{FACTS}} C^{\text{FACTS}}, \tag{45}$$

where $I_{k(i)}^{\max}$ is the maximum current on line $k(i)$, and FACTS ratings are calculated using the equation below [24]:

$$S_i^{\text{FACTS}} = V_i^{\max} I_{k(i)}^{\max} \approx V_i^{\max} f_{k(i)}^{\max}. \tag{46}$$

The device cost of PST deployment i is presented as follows [18]:

$$C_i^{\text{PST}} = f_{k(i)}^{\max} C^{\text{PST}}. \tag{47}$$

The unit costs of FACTS and PST devices are set at $150/kVA [25] and $100/kVA [18]. The ARR is calculated assuming a 10% RoR (110% gross return) and an interest rate of 6%. Additionally, the lifespan of the devices is considered to be 15 years.

The comparison between the AMR and the ARR for the 24-bus system is presented in Fig. 4. Results show that under the proposed market design, revenues of both GET deployments are much (1685% and 4362%) higher than

Table 4
Modifications to the 300-bus system

Branch No.	Capacity reduction (%)
61, 91, 101	60
115, 137, 365, 395	50
268	40

Table 5
GET allocation in the 300-bus system

GET	Location	Type	Operating limit
1	61	PST	10°
2	91	PST	10°
3	105	FACTS	0.03 pu
4	177	FACTS	0.03 pu
5	182	FACTS	0.03 pu
6	358	FACTS	0.03 pu

regulated returns calculated based on investments. This demonstrates the effectiveness of the proposed market design in incentivizing GET investments. Note that according to Lemma, 3 presented in Section 2, TGR will not exceed the savings created by GET operations. Therefore, considering the regulated RoR is much lower as shown in Fig. 4, the results reveal that GETs are significantly undervalued under the existing market structure. This highlights the importance of performance-based mechanisms similar to what is presented in this paper.

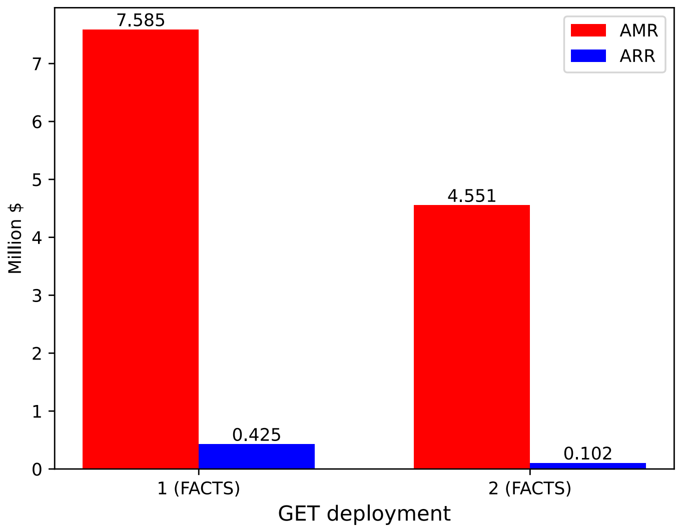

Figure 4: Comparison between AMR and ARR for GETs in the 24-bus system

3.2. 300-bus system

This part of the numerical studies is conducted to test the effectiveness of the proposed market design on a larger system, with more options for installation locations. GET deployments are increased and consist of different types of technologies. The system data are obtained from the IEEE 300-bus test case v23.07 in the IEEE PES power grid library (PGlib) [26]. Again, certain highly utilized branches have their thermal capacities reduced to increase congestion in the system. The modifications are shown in Table 4. GET allocation in the 300-bus system is presented in Table 5.

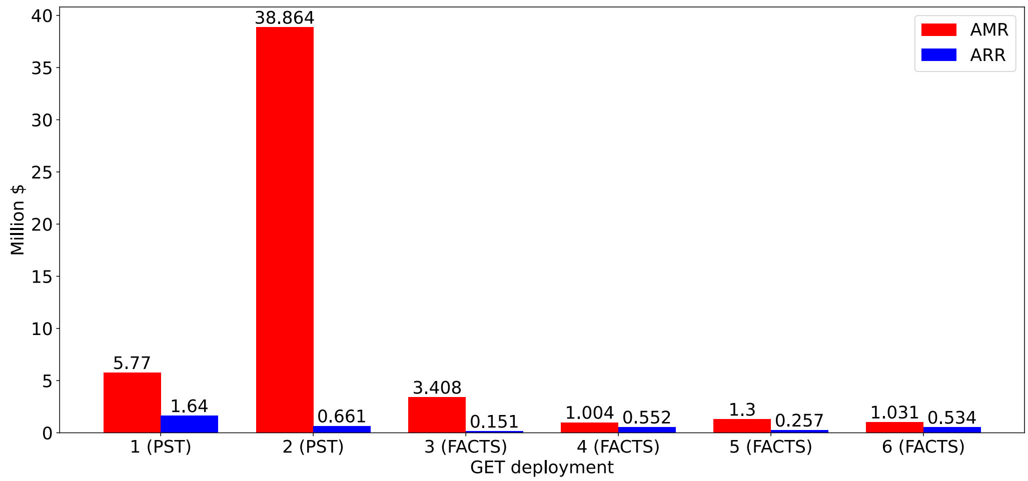

Figure 5: Comparison between AMR and ARR for GETs in the 300-bus system

AMR and ARR results are obtained following the same approach for the 24-bus system and are shown in Fig. 5. Again, the results show that for each of the GET deployments, AMR is much higher (up to 5780%) than ARR. GET investors will collect more revenue under the proposed market design than a regulated RoR. Additionally, GET deployments at different locations can belong to the same asset owner, and the summation of their revenues will be the total revenue of the owner. It is worth noting that the GET revenues of different deployments display a disparity. This is because certain locations are much more effective than others regarding GET placement. For example, Fig. 5 shows that GET deployment 2 (PST) is getting a much higher AMR than other GET deployments. It shows the importance of GET planning from the investors' perspective under the proposed market design as placing GETs at effective locations leads to higher revenues. Further discussion on this topic is presented later in this section.

3.3. Discussions

The numerical results show that, under the proposed market design, investors get more attractive financial rewards than the regulated RoR. The results also confirm that the market is revenue adequate. Further discussions about key topics on the impact and effectiveness of the proposed market design are presented in this subsection.

3.3.1. Robustness and scalability

The proposed market design is developed based on a generic DCOPF formulation. Its market properties are, thus, robust against variations in load level, system topologies, and congestion patterns, including the ones caused by RES uncertainties. Moreover, the payoffs to GET owners are calculated based on hourly system operation where the capacities of RES generation have been determined in the day-ahead unit commitment and hour-ahead markets. The same principles can be used for real-time market design and operation. Therefore, RES integration does not affect the operation of the proposed market design, and its effectiveness can be expected when implemented on systems under RES penetration. Additionally, the calculation of GET revenues is based on available shadow prices from DCOPF with linear GET modeling, thus ensuring computational efficiency and scalability when the proposed market design is implemented on larger systems.

3.3.2. Types of GETs

Different types of GETs can serve the purpose of congestion alleviation. However, the mathematical representation of GETs in power system optimization problems varies depending on the transmission system parameters they regulate and operating principles. This paper focuses on power flow controllers with linear modeling in DC power flow. Other types of GETs, including DLR, variance-impedance FACTS, and TS, have different types of modeling, some of which involve nonlinearity. For example, variable-impedance FACTS and TS can be modeled with mixed-integer linear constraints in DC power flow [19, 27]. Therefore, the derivation of marginal prices and the mathematical proof of revenue adequacy can be different from the methods presented in this paper. Future work will focus on incorporating various types of GETs into market operation frameworks similar to the one proposed in this paper, allowing efficient methods to be established to provide GET owners with adequate financial incentives.

3.3.3. Implementation and impacts

Under the proposed market design, GET revenues are calculated based on DCOPF solutions in a single time period, allowing for implementation in both day-ahead and real-time markets. It is worth noting that two aspects are important for the implementation of the proposed market design. First, it is essential to incorporate GET operation into power system operation. GET setpoints need to be co-optimized with generation dispatch in power system operation models, as demonstrated in the DCOPF formulation in Section 2, to fully utilize the capabilities of GETs and allow the marginal prices to be derived. The adoption of GETs is currently limited due to key barriers including the lack of proper incentives [2]. As mentioned previously, the proposed market design helps address this major challenge and facilitates the adoption of GETs in power system operations. Implementation of the proposed market design requires changing the regulatory structure around transmission upgrade. Moreover, the Federal Energy Regulatory Agency will need to be involved and make rules for how the proposed design can be integrated within established electricity markets. Second, the proposed market design is a system operation method, meaning that its results are based on already conducted GET planning processes. Optimal allocation is essential to the effectiveness of GET deployment, with various methods proposed by previous research [28, 29, 30]. As shown in Section 2, the total financial rewards to GET operation do not exceed the savings it creates, and over-investments can lead to zero payoffs. Therefore, in general, the proposed market design is expected to incentivize efficient and optimal GET planning, as it benefits both system operation and GET owners. Future work will focus on providing more detailed studies on how the proposed market design impacts the GET planning processes.

4. Conclusion

Proper incentives are vital to increasing grid-enhancing technologies (GETs) deployment in the power grid for transfer capability enhancements. This paper presents a market design that provides financial compensation to GET operations. The proposed mechanism is simple, straightforward, and based on integrating GETs in power system operation models. GET revenues under the proposed structure are calculated using the marginal prices associated with GET operation constraints and are settled along with generation dispatch. Simulation studies show that GET owners can collect a fair amount of revenues significantly higher than the regulated returns. The proposed market design is expected to provide significant incentives to GET investments. Future research will focus on integrating other types of GETs with nonlinear modeling into the proposed market design. The formulation along with the promising results, presented in the paper, suggest that system operators, GETs developer, and regulatory agencies should work together to adopt market-based mechanisms for GETs compensation.

A. Details of matrices

In this appendix, we show the construction of some of the matrices in P0 by showing detailed definitions of their elements.

First, the incidence matrix $\mathbf{A}$:

$$\mathbf{A}_{kn} = \begin{cases} -1 & \text{if } n = \text{to}(k) \\ 1 & \text{if } n = \text{fr}(k) \\ 0 & \text{else} \end{cases}, \quad n \in N, k \in K. \tag{48}$$

Second, the generator location matrix $\mathbf{\Gamma}$:

$$\mathbf{\Gamma}_{ng} = \begin{cases} 1 & \text{if } n(g) = n \\ 0 & \text{else} \end{cases}, \quad n \in N, g \in G. \tag{49}$$

Finally, the GET placement matrix $\mathbf{\Psi}$:

$$\mathbf{\Psi}_{ki} = \begin{cases} 1 & \text{if } k(i) = k \\ 0 & \text{else} \end{cases}, \quad k \in K, i \in \mathcal{G}. \tag{50}$$

B. Proof of Lemma 4

Lemma 4: the following equation regarding the ISF matrix and the incidence matrix holds:

$$\mathbf{\Phi}\mathbf{A}^{\mathrm{T}}\mathbf{\Phi} = \mathbf{\Phi}. \tag{51}$$

Proof: Lemma 4 is proved if the following equation holds:

$$\mathbf{\Phi}^{\mathrm{T}}\mathbf{A}\mathbf{\Phi}^{\mathrm{T}} = \mathbf{\Phi}^{\mathrm{T}}. \tag{52}$$

Let $|N|$ and $|K|$ denote the total number of buses and branches in the system, respectively. We set bus $|N|$ as the reference bus without losing genericity. Then, by definition, $\mathbf{\Phi}$ is presented as follows:

$$\mathbf{\Phi}_{|K|\times|N|} = \left[\begin{array}{c:c} \mathbf{\Phi'}_{|K|\times(|N|-1)} & \mathbf{0} \end{array}\right], \tag{53}$$

where $\mathbf{\Phi'}$ is the reduced ISF matrix developed by removing column $|N|$ of $\mathbf{\Phi}$. Elements in column $|N|$ of $\mathbf{\Phi}$, which is the column associated with the reference bus, are all zeroes as shown in (53). Based on DC power flow, matrix $\mathbf{\Phi'}$ is calculated using the following equation:

$$\mathbf{\Phi'} = \mathbf{B}_{\text{branch}}\mathbf{A'}\mathbf{B'}^{-1}, \tag{54}$$

We now present the development of each of the matrices on the right-hand side of (54). Matrix $\mathbf{A'}$ is developed by removing the column associated with the reference bus from $\mathbf{A}$. The relationship between $\mathbf{A}$ and $\mathbf{A'}$ is shown as follows:

$$\mathbf{A} = \left[\begin{array}{c:c} \mathbf{A'} & \mathbf{a'}_{|N|} \end{array}\right]. \tag{55}$$

Matrix $\mathbf{B'}_{(|N|-1)\times(|N|-1)}$ can be developed from the admittance matrix [31] $\mathbf{Y}_{|N|\times|N|}$ by first constructing $\mathbf{B}$ with neglecting the resistances and removing the imaginary units, as shown in (56). Note that $\mathbf{Y}$ does not have shunt terms.

$$\mathbf{Y} = j\mathbf{B}. \tag{56}$$

Then, the column and row associated with the reference bus in $\mathbf{B}$, which are bus $|N|$ and column $|N|$ in this case, are removed. $\mathbf{B}_{\text{branch}_{|K|\times|K|}}$ is a diagonal matrix with the diagonal elements being the susceptance of the lines.

We first present a proof of the invertibility of $\mathbf{B'}$. The rank of matrix $\mathbf{Y}$ is shown as follows [32, 33]:

$$\text{rank}(\mathbf{Y}) = |N| - 1. \tag{57}$$

Therefore, the rank of matrix $\mathbf{B}$ can be determined based on (56):

$$\text{rank}(\mathbf{B}) = \text{rank}(\mathbf{Y}) = |N| - 1. \tag{58}$$

Based on how $\mathbf{B'}$ is developed form $\mathbf{B}$, the following equation can be formulated:

$$\mathbf{B'} = \tilde{\mathbf{I}}^{\mathrm{T}}\mathbf{B}\tilde{\mathbf{I}}, \tag{59}$$

where $\tilde{\mathbf{I}}$ is defined as follows:

$$\tilde{\mathbf{I}}_{|N|\times(|N|-1)} = \left[\begin{array}{c} \mathbf{I}_{(|N-1|)\times(|N-1|)} \\ \hdashline \mathbf{0}^{\mathrm{T}} \end{array}\right]. \tag{60}$$

We can then formulate the following inequality using the Frobenius inequality:

$$\text{rank}(\mathbf{B'}) \geq \text{rank}(\tilde{\mathbf{I}}^{\text{T}}\mathbf{B}) + \text{rank}(\mathbf{B}\tilde{\mathbf{I}}^{\text{T}}) - \text{rank}(\mathbf{B}) = 2\text{rank}(\tilde{\mathbf{I}}^{\text{T}}\mathbf{B}) - \text{rank}(\mathbf{B}), \tag{61}$$

where $\text{rank}(\tilde{\mathbf{I}}^{\text{T}}\mathbf{B})$ satisfies the following inequality based on the Sylvester's rank inequality:

$$\text{rank}(\tilde{\mathbf{I}}^{\text{T}}\mathbf{B}) \geq \text{rank}(\tilde{\mathbf{I}}^{\text{T}}) + \text{rank}(\mathbf{B}) - |N| = |N| - 2. \tag{62}$$

The equality in (62) holds if and only if the following equation is satisfied [34]:

$$\tilde{\mathbf{I}}^{\text{T}}\mathbf{B} = \mathbf{O}. \tag{63}$$

The equation above does not hold as the diagonal elements of $\mathbf{B}$ are non-zero. Therefore, the rank of $\tilde{\mathbf{I}}^{\text{T}}\mathbf{B}$ satisfies the inequality shown as follows:

$$|N| - 1 \geq \text{rank}(\tilde{\mathbf{I}}^{\text{T}}\mathbf{B}) > |N| - 2, \tag{64}$$

which determines that $\text{rank}(\tilde{\mathbf{I}}^{\text{T}}\mathbf{B})$ is $|N| - 1$. We can now use this result in (61), which leads to:

$$\begin{aligned}\text{rank}(\mathbf{B'}) &\geq 2\text{rank}(\tilde{\mathbf{I}}^{\text{T}}\mathbf{B}) - \text{rank}(\mathbf{B}) \\ &= 2(|N| - 1) - (|N| - 1) \\ &= |N| - 1.\end{aligned} \tag{65}$$

Therefore, $\mathbf{B'}$ is full rank and invertible.

Eqn. (54) can be reformulated as:

$$\mathbf{A'}^{\text{T}}\mathbf{\Phi'}\mathbf{B} = \mathbf{A'}^{\text{T}}\mathbf{B}_{\text{branch}}\mathbf{A'}. \tag{66}$$

Let $\mathbf{S}$ denote the right-hand side of (66), we then have:

$$\begin{aligned}\mathbf{S} &= \begin{bmatrix}\tilde{\mathbf{a'}}_1 & \tilde{\mathbf{a'}}_2 & \dots & \tilde{\mathbf{a'}}_{|K|}\end{bmatrix} \begin{bmatrix} b_1 & 0 & \dots & 0 \\ 0 & b_2 & \dots & 0 \\ \vdots & & \ddots & \vdots \\ 0 & \dots & & b_{|K|}\end{bmatrix} \begin{bmatrix}\tilde{\mathbf{a'}}_1^{\text{T}} \\ \tilde{\mathbf{a'}}_2^{\text{T}} \\ \vdots \\ \tilde{\mathbf{a'}}_{|K|}^{\text{T}}\end{bmatrix} \\ &= \sum_{i=1}^{|K|} b_i \tilde{\mathbf{a'}}_i \tilde{\mathbf{a'}}_i^{\text{T}}.\end{aligned} \tag{67}$$

Then, we define a series of matrices as follows:

$$\mathbf{X}_i = b_i \tilde{\mathbf{a'}}_i \tilde{\mathbf{a'}}_i^{\text{T}}, i = 1, 2, \dots, |K|. \tag{68}$$

Based on the definition of $\mathbf{A}$, elements of matrix $\mathbf{X}$ in this series can be shown as follows:

$$(\mathbf{X}_k)_{ij} = \begin{cases} b_k & \text{if } i = j \text{ \& } i, j \in \{\text{to}(k), \text{fr}(k)\} \\ -b_k & \text{if } i \neq j \text{ \& } i, j \in \{\text{to}(k), \text{fr}(k)\} \\ 0 & \text{else} \end{cases} \tag{69}$$

$\mathbf{S}$, as shown in (67), is the summation of matrices $\mathbf{X}$. Therefore, its elements can be shown as follows:

$$\begin{aligned}&z_k \in \{0, 1\}, \\ &\text{if } i = j \ :\end{aligned} \tag{70}$$

$$S_{ij} = \sum_{k=1}^{|K|} z_k b_k, z_k = 1 \text{ iff } i \in \{\text{to}(k), \text{fr}(k)\}, \tag{71}$$

if $i \neq j$:

$$S_{ij} = \sum_{k=1}^{|K|} -z_k b_k, z_k = 1 \text{ iff } i, j \in \{\text{to}(k), \text{fr}(k)\}, \tag{72}$$

which is exactly how matrix $\mathbf{B}$ is defined. Therefore, we have proven that:

$$\mathbf{A'}^{\mathrm{T}} \mathbf{\Phi'} \mathbf{B'} = \mathbf{B'}. \tag{73}$$

Eqn. (73) is equivalent to:

$$\mathbf{\Phi'}^{\mathrm{T}} \mathbf{A'} = \mathbf{I}. \tag{74}$$

Then, calculation of $\mathbf{\Phi}^{\mathrm{T}}\mathbf{A}$ can be shown as follows:

$$\mathbf{\Phi}^{\mathrm{T}}\mathbf{A} = \left[\begin{array}{c} \mathbf{\Phi'}^{\mathrm{T}} \\ \hdashline \mathbf{0}^{\mathrm{T}} \end{array} \right] \left[\begin{array}{c:c} \mathbf{A'} & \mathbf{a'}_{|N|} \end{array} \right] = \left[\begin{array}{c:c} \mathbf{I} & \mathbf{\Phi'}^{\mathrm{T}} \mathbf{a'}_{|N|} \\ \hdashline \mathbf{0}^{\mathrm{T}} & 0 \end{array} \right]. \tag{75}$$

The left-hand side of (52) can be calculated using (53) and (75) as follows:

$$\begin{aligned} \mathbf{\Phi}^{\mathrm{T}}\mathbf{A}\mathbf{\Phi}^{\mathrm{T}} &= \left[\begin{array}{c:c} \mathbf{I} & \mathbf{\Phi'}^{\mathrm{T}} \mathbf{a'}_{|N|} \\ \hdashline \mathbf{0}^{\mathrm{T}} & 0 \end{array} \right] \left[\begin{array}{c} \mathbf{\Phi'}^{\mathrm{T}} \\ \hdashline \mathbf{0}^{\mathrm{T}} \end{array} \right] \\ &= \left[\begin{array}{c} \mathbf{I}\mathbf{\Phi'}^{\mathrm{T}} \\ \hdashline \mathbf{0}^{\mathrm{T}} \end{array} \right] = \left[\begin{array}{c} \mathbf{\Phi'}^{\mathrm{T}} \\ \hdashline \mathbf{0}^{\mathrm{T}} \end{array} \right] = \mathbf{\Phi}^{\mathrm{T}}. \end{aligned} \tag{76}$$

Therefore, (52) holds, which proves Lemma 4.

Acknowledgements

This document is the results of the research projects funded by the National Science Foundation grant number 2146531.

References

[1] U.S. Department of Energy, Grid enhancing technologies - A case study on ratepayer impact (Feb. 2022).
URL `https://www.energy.gov/sites/default/files/2022-04/Grid%20Enhancing%20Technologies%20-%20A%20Case%20Study%20on%20Ratepayer%20Impact%20-%20February%202022%20CLEAN%20as%20of%20032322.pdf`

[2] O. Mirzapour, X. Rui, M. Sahraei-Ardakani, Grid-enhancing technologies: Progress, challenges, and future research directions, Electr. Power Syst. Res. 230, Art. no. 110304 (May 2024).

[3] O. Mirzapour, X. Rui, M. Sahraei-Ardakani, Transmission impedance control impacts on carbon emissions and renewable energy curtailment, Energy 278, Art. no. 127741 (Sep. 2023).

[4] M. Sahraei-Ardakani, Merchant power flow controllers, Energy Econ. 74 (2018) 878–885.

[5] Allsup, Maeve and Jenkins, Lisa Martine, DOE: Utilities must act now to unlock latent grid capacity, Latitude Media, (Apr. 2024).
URL `https://www.latitudemedia.com/news/doe-utilities-must-act-now-to-unlock-latent-grid-capacity`

[6] Jay Caspary, The role for grid-Enhancing technologies, *Energy Systems Information Group* (Jan. 2022).
URL `https://www.esig.energy/the-role-for-grid-enhancing-technologies/`

[7] K. Rebane, K. Siegner, S. Toth, Cheaper, cleaner, faster - Four strategies utility regulators can use to accelerate new renewables interconnection., *RMI* (July 2023).
URL `https://rmi.org/cheaper-cleaner-faster/`

[8] X. Rui, O. Mirzapour, B. Pruneau, M. Sahraei-Ardakani, A review of economic incentives for efficient operation of flexible transmission, in: 2023 North Amer. Power Symp., IEEE, 2023, pp. 1–6.

[9] M. R. Hesamzadeh, J. Rosellón, S. A. Gabriel, I. Vogelsang, A simple regulatory incentive mechanism applied to electricity transmission pricing and investment, Energy Econ. 75 (2018) 423–439.

[10] J. Contreras, G. Gross, J. M. Arroyo, J. I. Muñoz, An incentive-based mechanism for transmission asset investment, Decis. Support Syst. 47 (1) (2009) 22–31.

[11] N. Mithulananthan, N. Acharya, A proposal for investment recovery of FACTS devices in deregulated electricity markets, Electr. Power Syst. Res. 77 (5-6) (2007) 695–703.
[12] WATT Coalition, Frequently asked questions about a shared savings incentive for grid enhancing technologies (2022).
URL https://watt-transmission.org/resources-2/shared-savings-faq/
[13] V. Asgharian, M. Abdelaziz, A low-carbon market-based multi-area power system expansion planning model, Electr. Power Syst. Res. 187, Art. no. 106500 (Oct. 2020).
[14] J. H. Roh, M. Shahidehpour, Y. Fu, Market-based coordination of transmission and generation capacity planning, IEEE Trans. Power Syst. 22 (4) (2007) 1406–1419.
[15] R. Hemmati, R.-A. Hooshmand, A. Khodabakhshian, Coordinated generation and transmission expansion planning in deregulated electricity market considering wind farms, Renewable Energy 85 (2016) 620–630.
[16] M. Sahraei-Ardakani, S. A. Blumsack, Transfer capability improvement through market-based operation of series FACTS devices, IEEE Trans. Power Syst. 31 (5) (2016) 3702–3714.
[17] X. Rui, M. Sahraei-Ardakani, T. R. Nudell, Linear modelling of series FACTS devices in power system operation models, IET Gener., Transmiss. Distri. 16 (6) (2022) 1047–1063.
[18] X. Zhang, D. Shi, Z. Wang, B. Zeng, X. Wang, K. Tomsovic, Y. Jin, Optimal allocation of series FACTS devices under high penetration of wind power within a market environment, IEEE Trans. Power Syst. 33 (6) (2018) 6206–6217.
[19] M. Sahraei-Ardakani, K. W. Hedman, Computationally efficient adjustment of FACTS set points in DC optimal power flow with shift factor structure, IEEE Trans. Power Syst. 32 (3) (2017) 1733–1740.
[20] C. Grigg, P. Wong, P. Albrecht, R. Allan, M. Bhavaraju, R. Billinton, Q. Chen, C. Fong, S. Haddad, S. Kuruganty, et al., The IEEE reliability test system-1996. a report prepared by the reliability test system task force of the application of probability methods subcommittee, IEEE Trans. Power Syst. 14 (3) (1999) 1010–1020.
[21] S. Diamond, S. Boyd, CVXPY: A Python-embedded modeling language for convex optimization, J. Mach. Learn. Res. 17 (83) (2016) 1–5.
URL http://jmlr.org/papers/v17/15-408.html
[22] Department of Electrical Engineering, University of Washington, Power systems test case archive.
URL http://labs.ece.uw.edu/pstca/rts/pg_tcarts.htm
[23] Y. Sang, M. Sahraei-Ardakani, The interdependence between transmission switching and variable-impedance series FACTS devices, IEEE Trans. Power Syst. 33 (3) (2017) 2792–2803.
[24] N. G. Hingorani, L. Gyugyi, FACTS Concept and General System Considerations, 2000, pp. 1–35. doi:10.1109/9780470546802.ch1.
[25] I. Zunnurain, Y. Sang, P. Mandal, M. Velez-Reyes, J. Espiritu, Improving the resilience of large-scale power systems using distributed static series compensators, Int. J. Elect. Power Energy Syst. 145, Art. no. 108702 (Feb. 2023).
[26] S. Babaeinejadsarookolaee, A. Birchfield, R. D. Christie, C. Coffrin, C. DeMarco, R. Diao, M. Ferris, S. Fliscounakis, S. Greene, R. Huang, et al., The power grid library for benchmarking AC optimal power flow algorithms, arXiv preprint arXiv:1908.02788 (2019).
[27] P. A. Ruiz, E. Goldis, A. M. Rudkevich, M. C. Caramanis, C. R. Philbrick, J. M. Foster, Security-constrained transmission topology control MILP formulation using sensitivity factors, IEEE Trans. Power Syst. 32 (2) (2017) 1597–1605.
[28] Y. Zhang, J. Wang, T. Ding, X. Wang, Conditional value at risk-based stochastic unit commitment considering the uncertainty of wind power generation, IET Gener., Transmiss. Distrb. 12 (2) (2018) 482–489.
[29] S. Talpur, T. Lie, R. Zamora, Application of dynamic thermal rating: Overhead line critical spans identification under weather dependent optimized sensor placement, Electric power systems research 180 (2020) 106125.
[30] O. Ziaee, F. Choobineh, Optimal location-allocation of tcscs and transmission switch placement under high penetration of wind power, IEEE Transactions on Power Systems 32 (4) (2016) 3006–3014.
[31] The DC power flow equations.
URL https://home.engineering.iastate.edu/~jdm/ee553/DCPowerFlowEquations.pdf
[32] A. M. Kettner, M. Paolone, On the properties of the power systems nodal admittance matrix, IEEE Trans. Power Syst. 33 (1) (2018) 1130–1131. doi:10.1109/TPWRS.2017.2719583.
[33] D. Turizo, D. K. Molzahn, Invertibility conditions for the admittance matrices of balanced power systems, IEEE Trans. Power Syst. 38 (4) (2023) 3841–3853. doi:10.1109/TPWRS.2022.3206285.
[34] N. Thome, Inequalities and equalities for $\ell = 2$ (Sylvester), $\ell = 3$ (Frobenius), and $\ell > 3$ matrices, Aequ. Math. 90 (2016) 951–960.